Neuropharmacology 90 (2015) 63–73

Contents lists available at ScienceDirect

Neuropharmacology

journal homepage: www.elsevier.com/locate/neuropharm

Characterizing new fluorescent tools for studying 5-HT$_3$ receptor pharmacology

Thomas Jack [a, 1], Jonathan Simonin [a, 1], Marc-David Ruepp [a, 1], Andrew J. Thompson [a, 1, 2], Jürg Gertsch [b], Martin Lochner [a, *]

[a] Department of Chemistry and Biochemistry, University of Bern, Freiestrasse 3, 3012 Bern, Switzerland
[b] Institute of Biochemistry and Molecular Medicine, University of Bern, Bühlstrasse 28, 3012 Bern, Switzerland

ARTICLE INFO

Article history:
Received 18 July 2014
Received in revised form
30 October 2014
Accepted 16 November 2014
Available online 22 November 2014

Keywords:
Cys-loop
5-HT$_3$ receptor
Fluorescence
Ligand binding
Flow cytometry
Fluorescence polarization

ABSTRACT

The pharmacological characterization of ligands depends upon the ability to accurately measure their binding properties. Fluorescence provides an alternative to more traditional approaches such as radioligand binding. Here we describe the binding and spectroscopic properties of eight fluorescent 5-HT$_3$ receptor ligands. These were tested on purified receptors, expressed receptors on live cells, or *in vivo*. All compounds had nanomolar affinities with fluorescent properties extending from blue to near infra-red emission. A fluorescein-derivative had the highest affinity as measured by fluorescence polarization (FP; 1.14 nM), flow cytometry (FC; 3.23 nM) and radioligand binding (RB; 1.90 nM). Competition binding with unlabeled 5-HT$_3$ receptor agonists (5-HT, *m*CPBG, quipazine) and antagonists (granisetron, palonosetron, tropisetron) yielded similar affinities in all three assays. When cysteine substitutions were introduced into the 5-HT$_3$ receptor binding site the same changes in binding affinity were seen for both granisetron and the fluorescein-derivative, suggesting that they both adopt orientations that are consistent with co-crystal structures of granisetron with a homologous protein (5HTBP). As expected, *in vivo* live imaging in anaesthetized mice revealed staining in the abdominal cavity in intestines, but also in salivary glands. The unexpected presence of 5-HT$_3$ receptors in mouse salivary glands was confirmed by Western blots. Overall, these results demonstrate the wide utility of our new high-affinity fluorescently-labeled 5-HT$_3$ receptor probes, ranging from *in vitro* receptor pharmacology, including FC and FP ligand competition, to live imaging of 5-HT$_3$ expressing tissues.

1. Introduction

High-affinity, radiolabeled 5-HT$_3$ receptor antagonists are commercially available and have been frequently used to characterize 5-HT$_3$ receptors in live cells and in *in vitro* binding assays (Barnes et al., 2009; Brady et al., 2001). However, fluorescent ligands can provide alternative opportunities for quantifying binding interactions using fast, economical and information rich methods that do not generate radioactive waste and can be more easily adapted to high-throughput technologies.

Fluorometric methods have been used in high-resolution microscopy to observe phenomena, such as the movement and internalization of cell-surface receptors, distances between fluorophores and the physical environments within proteins, among other uses (Lavis and Raines, 2008; Wysocki and Lavis, 2011). For quantitative cellular and molecular pharmacological measurements flow cytometry (FC) and fluorescence polarization (FP) can

Abbreviations: 5-HT, 5-hydroxytryptamine (serotonin); ACh, acetylcholine; FACS, fluorescence activated cell sorting; FC, flow cytometry; FLAG, peptide tag DYKDDDDK; FP, fluorescence polarization; G-AD, granisetron-acridone; G-CN, granisetron-coumarin; G-FL, granisetron-fluorescein; G-TMR, granisetron-5-tetramethylrhodamine; G-TO, granisetron-thiazole orange; G-RhB, granisetron-rhodamine B; G-R101, granisetron-rhodamine 101; G-SiR, granisetron-Si-rhodamine; *m*CPBG, *meta*-chlorophenylbiguanide; PTX, picrotoxin; RB, radioligand binding.

* Corresponding author. Tel.: +41 31 631 3311; fax: +41 31 631 4272.
E-mail addresses: thomas.jack@dcb.unibe.ch (T. Jack), jsimonin@dcb.unibe.ch (J. Simonin), marc.ruepp@dcb.unibe.ch (M.-D. Ruepp), ajt44@cam.ac.uk (A.J. Thompson), juerg.gertsch@ibmm.unibe.ch (J. Gertsch), martin.lochner@dcb.unibe.ch (M. Lochner).
[1] The authors made equal contributions to the study.
[2] Present address: Pharmacology Department, University of Cambridge, Tennis Court Road, Cambridge CB2 1PD, UK.

http://dx.doi.org/10.1016/j.neuropharm.2014.11.007
0028-3908/

be used. However, the challenge with these techniques is the creation of fluorescent tracers that have a sufficiently high affinity for the protein target and give suitable fluorescent signals that are sufficiently higher than background. Here, we use the 5-HT_3 receptor as a model system to test the utility of fluorophores conjugated to a competitive antagonist of this receptor.

The 5-HT_3 receptor is a ligand-gated ion channel related to nicotinic acetylcholine (nAChRs), γ-amino butyric acid ($GABA_A$) and glycine receptors (Thompson et al., 2010a). These receptors are referred to as the Cys-loop family and are located in the cell membranes of central and peripheral synapses where they are responsible for fast neurotransmission. All of these receptors consist of an extracellular domain, a transmembrane domain and an intracellular domain. When agonists bind to extracellular binding sites a conformational change opens a transmembrane pore, allowing ions to enter the cell. Compounds that compete at these sites and prevent opening of the pore are known as competitive antagonists, and several are marketed as antiemetic drugs that alleviate symptoms resulting from chemotherapy, radiotherapy and general anesthesia (Thompson and Lummis, 2007; Walstab et al., 2010). 5-HT_3 receptor competitive antagonists are also less frequently used to treat irritable bowel syndrome (IBS), and there is interest in partial agonists for treating the same disorder (Moore et al., 2013). There have also been suggestions that 5-HT_3 receptor antagonists could be used to control neurological disorders such as depression, drug abuse, schizophrenia, fibromyalgia, pruritus and pain (Thompson and Lummis, 2007; Walstab et al., 2010). Recent literature shows that new 5-HT_3 receptor ligands continue to be identified, with particular interest in allosteric modulators and sub-type selective ligands (Thompson and Lummis, 2013). These will inevitably require further pharmacological characterization and new tools to allow the efficient analysis of receptor binding will be useful.

Here we describe the spectroscopic and ligand binding properties of a wider range of nanomolar affinity fluorophores that use granisetron as a ligand scaffold. We provide mutagenesis data that shows (i) the fluorescent probes bind to the same site as the granisetron scaffold, (ii) describe two pharmacological assays (flow cytometry and fluorescence polarization) which give robust and reproducible results that are the same as those determined using radioligand methods, and (iii) show the utility of the fluorophores in determining the localization of receptors in *in vivo* imaging. As such, these results represent the first description of a molecular toolkit that encompasses the whole fluorescent spectrum, making it appealing for a broad range of 5-HT_3 receptor studies.

2. Experimental procedures

2.1. Chemicals & drugs

Granisetron, palonosetron and tropisetron were synthesized according to published procedures (Bermudez et al., 1990; Clark et al., 1993; Langlois et al., 1993; Vernekar et al., 2010). 5-HT (serotonin) creatinine sulfate, acetylcholine (ACh) chloride, quipazine maleate, γ-aminobutyric acid (GABA), glycine and picrotoxin (PTX; an equimolar mixture of picrotoxinin and picrotin) were obtained from Sigma Aldrich (St. Louis, MO, USA). *m*CPBG was from Tocris. Human 5-HT3A (Accession: 46098) subunit cDNA was kindly provided by J. Peters (Dundee University, UK). The synthesis of fluorescent granisetron derivatives G-CN, G-FL and G-RhB (Fig. 1A) was described previously (Simonin et al., 2012; Vernekar et al., 2010). Fluorescent granisetron conjugates G-SiR, G-TO, G-R101, G-TMR and G-AD (Fig. 1A) were synthesized accordingly (for detailed description of synthetic procedures, for full spectroscopic characterization and purity assessment see Supplementary data). Briefly, fluorophores were either purchased (rhodamine 101 and acridone; Sigma Aldrich) or synthesized according to published procedures (Egawa et al., 2011; Holzhauser et al., 2010; Kvach et al., 2009), and coupled to the granisetron core via linkers.

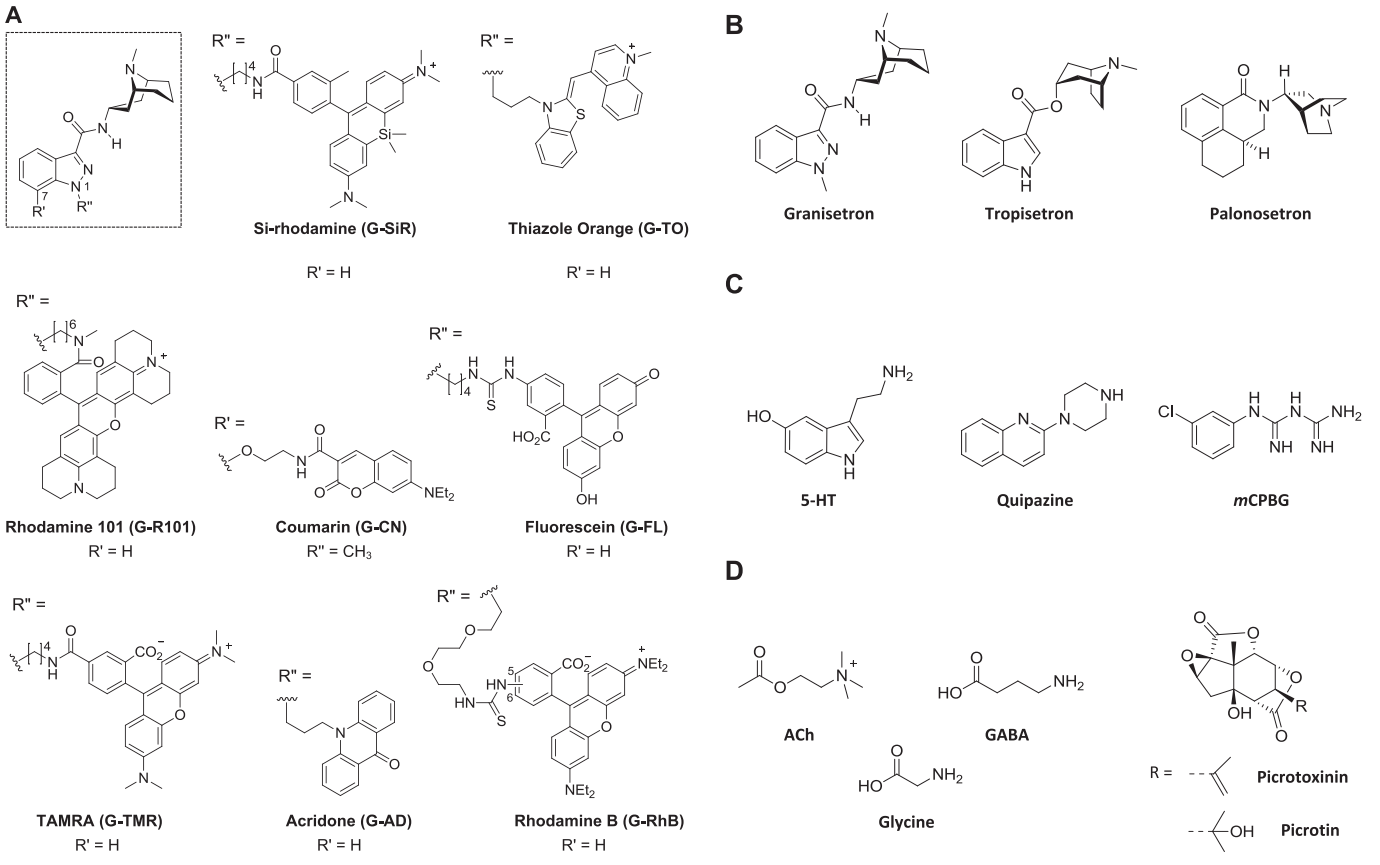

Fig. 1. A). Chemical structures of the fluorescent granisetron conjugates described here. Chemical structures of antagonists (B), agonists (C) and negative controls (D) used in competition assays.

2.2. Plasmids

A FLAG-myc-tagged human 5-HT3A subunit expression construct was created by fusion PCR and subsequent cloning into the XbaI and NotI sites of the lentiviral expression Vector pCDH-CuO-EF1-RFP (System Biosciences, CA, USA). The resulting cDNA coded for a double-tagged protein with the FLAG-tag (DYKDDDDK) inserted after amino acid 23 of the 5-HT_3 receptor, followed by the myc-tag, inserted after amino acid 29. The construct was verified by DNA sequencing. Mutagenesis was performed using the QuikChange method (Agilent Technologies Inc., California, USA).

2.3. Cell culture

Human embryonic kidney (HEK) 293T cells were grown in DMEM/F12 (Gibco, Life Technologies, CA, USA) supplemented with 10% fetal bovine serum (FBS; Bio-Concept, Allschwil, Switzerland) at 37 °C in a moist atmosphere containing 5% CO_2.

2.4. In vivo imaging

C57BL male mice (6–10 weeks old, 20–25 g body weight) were housed under standard environmental conditions ($n = 5$ per cage) at 22–24 °C under a 12 h–12 h light–dark cycle supplied with food and water ad libitum. Mice were anesthetized and shaved carefully on their underside and immediately injected i.p. with 5 mg/kg of G-SiR dissolved in DMSO in an injection volume of 15 μl. After 5, 10, 20 min and 1 h images were recorded in a IVIS Lumina II instrument (Caliper Life Sciences) using filter set 3 (excitation 615–665 nm; emission 695–770 nm) at 37 °C. Control mice were injected with vehicle (DMSO). Upon completion of the experiments the mice were sacrificed and organs dissected. Images were obtained in 3 independent experiments. Animals were handled in accordance with the Code of Ethics of the Directive 2010/63/EU.

2.5. Virus production

FuGene HD (Promega, WI, USA) was used to transfect HEK 293T cells with pCDH-CuO-FLAG-myc-5HT_3-EF1-RFP, pCMVΔR8.91 and pMD2.G according to established methods (Wiznerowicz and Trono, 2003). Lentiviral supernatants were collected 48, 72 and 96 h post transfection and filtered through a 0.45 μM polyethersulfone sterile filter (Millipore Corp, MA, USA). For transduction, HEK 293T cells were incubated with lentiviral supernatants supplemented with 5 μg mL^{-1} polybrene (hexadimethrine bromide, Sigma Aldrich). After 7 h, polybrene was diluted to 2.5 μg mL^{-1} by the addition of fresh DMEM/10% FBS, and the procedure repeated for two days. After expansion of the transduced cells, highly RFP positive cells were collected by fluorescence-activated cell sorting (FACS) to yield a highly transduced cell pool.

2.6. Protein purification

HEK 293T cells stably expressing FLAG-myc-5-HT_3 receptor were grown as monolayers in T300 plates. At a density of 80%, cells were washed once with phosphate buffered saline (PBS (mM); 0.1 NaCl, 2.0 Na_2HPO_4, 0.54 KCl, 0.4 KH_2PO_4, pH 7.4), mechanically detached into PBS, collected by centrifugation at 500 g for 5 min, snap frozen in liquid N_2 and stored at −70 °C until needed. After defrosting, cells were diluted with 2 mL Tris–EDTA (50 mM Tris–HCl, 0.5 mM EDTA, pH 7.5) containing Halt Protease Inhibitor (Pierce, Thermo Scientific, IL, USA) and homogenized with a 5 mL cell-douncer, followed by trituration through 21-gauge and 27-gauge needles. Soluble proteins were removed by centrifugation at 100,000 *g* for 30 min, and the membrane fraction dissolved in 10 mL PBS + 2 mM $C_{12}E_9$, before being incubated head-over-tail for 1 h at 4 °C; a concentration of the micelle forming polyether that is higher than the critical micelle concentration (Privé, 2007). Insoluble fractions were removed by centrifugation at 100,000 *g* for 1 h and the supernatant incubated with anti-FLAG M2 agarose beads (Sigma Aldrich), head-over-tail for 2 h at 4 °C. Bound beads were washed 5× with PBS + 2 mM $C_{12}E_9$ and protein recovered by incubating with 250 μL PBS + 0.4 mM $C_{12}E_9$ supplemented with 1 mg mL^{-1} FLAG peptide (Pepnome Ltd, Zhuhai, China) for 30 min. The eluate was recovered by centrifugation of the suspension through Micro Bio-Spin columns (Bio-Rad, California, USA) at 500 g for 1 min. This was dialyzed with a 10 K MWCO Slide-A-Lyzer (Thermo Scientific, Waltham, MA, USA) overnight in PBS + 0.4 mM $C_{12}E_9$, aliquoted, snap frozen in liquid N_2 and stored at −70 °C.

2.7. Protein purity & quantification

To determine purity and yield of 5-HT_3 receptors from transfected HEK 293 cells, 20 μL of the eluate and pepsin standards were subjected to SDS-Page on a 4–12% NuPAGE Novex Bis-Tris gel (Life Technologies), followed by colloidal Coomassie staining, imaging and quantification using a LI-COR Odyssey infrared system (LI-COR Biosystems, NE, USA). To verify the results of Coomassie staining, samples were subjected to amino acid analysis using HPLC (column Novapack C18, 60 Å, 3.9 × 150 mm) after hydrolysis in 6 M HCl.

For Western blotting, proteins were transferred to a 0.22 μM nitrocellulose membrane using the iBlot Dry Blotting System (Invitrogen, CA, USA). Membranes were blocked for 1 h in TBS (50 mM Tris–Cl, 150 mM NaCl, pH 7.5) containing 0.1% Tween-20 and 5% skimmed milk powder, before incubating with the 1° antibodies goat anti-FLAG (1:3000, Bethyl Laboratories, Montgomery, USA) and mouse anti-myc (1:500, Invitrogen) in TBS-tween-milk overnight at 4 °C. Membranes were washed 5× for 5 min each with TBS-tween and incubated for 2 h at room temp with the 2° antibodies donkey anti-goat IRDye800 (1:10,000, Li-Cor) and donkey anti-mouse IRDye680 (1:10,000, LI-COR) in TBS-tween-milk at room temp. After 5× washes with TBS-tween, membranes were scanned using the Odyssey Imaging System (LI-COR).

To determine the expression of 5-HT_3 receptors in mouse, total protein lysates from brain, colon, skeletal muscle, salivary gland mandibular and salivary gland parotid were purchased from Zyagen (San Diego, CA, USA), mixed 1:1 with 2× LDS buffer and boiled for 25 min at 60 °C and 37.5 μg total protein lysate loaded on 3–8% NuPage Tris-Acetate gels. Proteins were transferred to nitrocellulose and incubated over night at 4 °C with goat anti-5-HT_3 (Santa Cruz, sc-19152, 1:100 in TBS-Tween-Milk) followed by Donkey anti-Goat IRDye800CW (LI-COR, 1:10′000 in TBS-Tween-Milk) for 1.5 h at room temperature.

2.8. Fluorescence polarization

Purified 5-HT_3 receptors were quantified as described above and a molarity calculated using a molecular weight of 276 kDa (calculated using the online tool ExPASy PeptideMass). Concentrations of purified 5-HT_3 receptor were prepared in PBS + 2 mM $C_{12}E_9$ on ice. 2 nM of fluorescent ligand was added in a total volume of 25 μL/well in NUNC 384-well flat bottom black plates (Greiner Bio-One Ltd, Stonehouse, UK) and incubated for 1 h in the dark at room temp. Polarization was measured with a FARCyte Ultra Plate Reader (Tecan Gp LTS, Männedorf, Switzerland) with 485 nm excitation and 535 nm emission, gain fixed at 100 and the Z-position optimized. For the measurement of non-specific binding a saturating concentration of either granisetron (10 μM) or quipazine (1 mM) was added, with both giving similar results. Raw data were processed using the integrated XFLUOR4 v4.51 software. Competition measurements were made by incubating compounds (0.01 nM–100 μM) with 3 nM 5-HT_3 receptor and 2 nM fluorescent ligand using the same setup.

2.9. Flow cytometry

HEK 293T cells stably expressing the 5-HT_3 receptor were grown in monolayers and harvested from a 90 mm culture dish using 10 mL 1:250 Trypsin-EDTA (Amimed) for 10 min at 37 °C. The digestion was terminated by the addition of 25 mL DMEM + 10% FBS and cells pelleted at low speed for 2 min. The pellet was resuspended in 3 mL PBS containing 10 mM EDTA, 1 mM $MnSO_4$ and 50 U mL^{-1} Cyanase (RiboSolutions, Inc, Cedar Creek, TX, USA) (PBS-EMC). Cells were filtered through a cell strainer (BD Falcon, Franklin Lakes, NJ, USA) and, for saturation studies, incubated with 0.1 nM–20 μM G-FL in the presence or absence of 1 mM quipazine or 10 μM granisetron for 15 min at room temperature; for competition studies varied concentrations of non-labeled ligands were co-incubated with 10 nM G-FL. Cells were pelleted and washed in PBS-EMC containing 50 μg mL^{-1} bovine serum albumin, before being resuspended in the same buffer and analyzed on a FACScan flow cytometer (Becton Dickinson, Franklin Lakes, NJ, USA), equipped with a solid state laser from Cytek (Cambridge, UK) at 485 nm excitation/535 nm emission, running the integrated CellQuest Pro software.

2.10. Radioligand binding

Saturation binding (8 point) curves were determined by incubating crude extracts of HEK 293T cells stably expressing 5-HT_3 receptors in 0.5 mL HEPES buffer (pH 7.4) containing 0.1–20 nM [^{3}H]granisetron. Competition binding (10 point) was determined by incubating the same cell extracts in 0.5 mL HEPES buffer (pH 7.4) containing 0.75 nM [^{3}H]granisetron and differing concentrations of competing ligands. Non-specific binding was determined with 1 mM quipazine or 10 μM tropisetron which gave similar results. Incubations were terminated by filtration onto Whatman GF/B filters (Sigma Aldrich) and radioactivity measured using a Tri-Carb 2100TR (Perkin Elmer, Waltham, MA, USA) scintillation counter.

2.11. Data analysis

All data analysis was performed with GraphPad Prism v5.00 (GraphPad Software, San Diego, CA, USA). For FC, FP and RB saturation experiments, data were analyzed by iterative curve-fitting according to:

$$y = \frac{A_{\max} \cdot [L]}{K_d + [L]} \quad (1)$$

where y is bound ligand, $A_{\max}$ is the maximum signal at equilibrium, K_d is the equilibrium dissociation constant, and $[L]$ is the free concentration of labeled ligand.

FC, FP and RB competition data were analyzed by iterative curve fitting according to:

$$y = A_{\min} \frac{A_{\max} - A_{\min}}{1 + 10^{[L] - \log IC_{50}}} \quad (2)$$

where A_{min} is the minimum signal, A_{max} is the maximum signal, [L] is the concentration of competing ligand and IC_{50} the concentration of competing ligand that blocks half the signal.

K_i values were determined from the IC_{50} values using the Cheng–Prusoff equation:

$$K_i = \frac{IC}{1 + [L]/K_d} \quad (3)$$

where K_i is the equilibrium dissociation constant for binding of the unlabeled ligand, [L] is the concentration of labeled ligand and K_d is the equilibrium dissociation constant of the labeled ligand.

Kinetic parameters were determined according to the following model of a simple bimolecular binding scheme:

$$L + R \underset{k_{off}}{\overset{k_{on}}{\rightleftharpoons}} LR \quad (4)$$

where L is the free ligand concentration, R is receptor concentration, LR is the ligand–receptor complex and k_{on} and k_{off} are the microscopic association and dissociation rate constants. In a simple scheme such as this, the equilibrium dissociation constant (K_d) is equal to the ratio of dissociation to association rate constants, such that:

$$K_d = \frac{k_{off}}{k_{on}} \quad (5)$$

Dissociation was measured by allowing labeled ligands to reach equilibrium and then adding a final concentration of 1 mM quipazine (~$K_d \times 10^6$) for varying time periods. Dissociation data were fitted to either a single or double exponential decay to yield k_{off}. To determine the association rate (k_{on}), the observed association rate (k_{obs}) was measured for a range of labeled ligand concentrations. The experiment was started ($t = 0$) by the addition of labeled ligand and the signal measured at varying time points to construct association curves. Association curves were fitted to a single exponential association to calculate k_{obs}, which is a product of both the rates k_{on} and k_{off}. If k_{obs} is plotted against the ligand concentration, according to the simple model (4), the slope of this plot equals the association constant (k_{on}) and the y-intercept of this line (at $x = 0$) is the dissociation constant (k_{off}). k_{on} can also be calculated as described by Hill (1909), where k_{off} is predetermined from ligand dissociation rate experiments.

$$k_{on} = \frac{k_{obs} - k_{off}}{[L]} \quad (6)$$

All values in the manuscript are shown as the mean ± sem of independent experimental measurements.

3. Results

3.1. Properties of fluorophores

We have synthesized a series of 5-HT_3 receptor ligands containing a granisetron scaffold conjugated to diverse fluorophores (Figs. 1 and 2). A summary of their spectral and binding properties is shown in Tables 1 and 2. Competition of [^{3}H]granisetron with varied concentrations of these fluorescent granisetron-derivatives revealed nanomolar affinities for all compounds, with the highest affinity shown by the fluorescein derivative G-FL. Quantum yields and molar extinction coefficients were generally high, giving strong fluorescent intensities. These results clearly show that large moieties can be attached to positions N1 and C7 of granisetron without loss of binding.

3.2. Effects of mutating the 5-HT_3 receptor binding site

Granisetron has been co-crystallized with 5HTBP, a homologue of the 5-HT_3 receptor extracellular domain (Kesters et al., 2013). To determine if G-FL binds in a similar location and orientation we made a series of cysteine mutations within four of the six recognized binding loops of the 5-HT_3 receptor and measured both G-FL and granisetron binding. These mutations were in loops A (L126C, N128C), B (T179C, W183C), D (R92C, W90C) and E (Y141C, Q151C) which were chosen as they show more sequence conservation than the two remaining loops C and F.

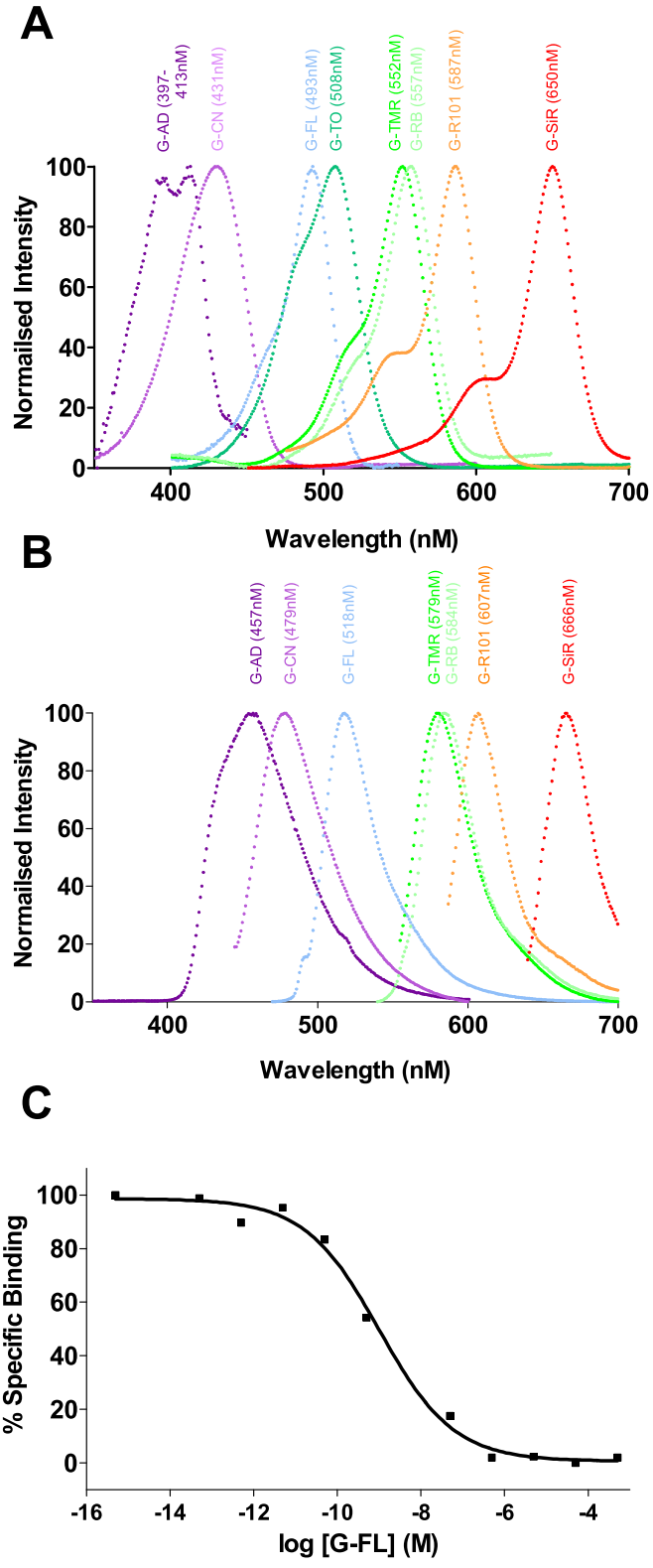

Fig. 2. Properties of fluorescent ligands. Absorption (A) and emission (B) spectra of fluorescent granisetron-derivatives. (C) Radioligand competition binding of G-FL with 0.75 nM [^{3}H]granisetron, a radiolabeled form of the scaffold to which the fluorophores were conjugated.

Table 1
Spectroscopic and binding properties of granisetron fluorophore conjugates.

Compound name	Absorption peak (nm)	Emission peak (nm)	Φ_F	ε (M^{-1} cm^{-1})	pK_i[a] (n) (M)	K_i (nM)
G-AD	397–413	457	1	1000	6.49 ± 0.05 (3)	323
G-CN[b]	431	479	0.02	40,100	8.24 ± 0.01 (3)	5.75
G-FL[b]	493	518	0.69	45,000	8.72 ± 0.07 (3)	1.90
G-TO	508	–	–	34,030	6.67 ± 0.20 (4)	214
G-TMR	552	579	0.54	52,550	7.56 ± 0.04 (3)	27.5
G-RhB[b]	557	584	0.24	53,100	6.13 ± 0.07 (3)	741
G-R101	587	607	0.54	57,900	7.66 ± 0.04 (4)	21.9
G-SiR	650	666	0.47	92,660	8.48 ± 0.27 (4)	3.31

[a] Measured using radioligand competition with [^{3}H]granisetron. ε = molar extinction coefficient measured in PBS. Φ_F = quantum yield of fluorescence. Values were determined using the methods described in Simonin et al. (2012). G-TO is self-quenching and only emits fluorescence when bound to 5-HT$_3$ receptor.
[b] Taken from Simonin et al. (2012). Fluorophores are: AD, acridone; CN, coumarin; FL, fluorescein; TO, thiazole orange; TMR, 5-TAMRA; RhB, Rhodamine B; R101, Rhodamine 101; SiR, Si-rhodamine. Brightness = $\Phi_F \times \varepsilon$ (Lavis and Raines, 2008). All measurements were made in PBS.

The locations of the substitutions and the affinities of the mutant receptors are shown in Fig. 3. With G-FL five of the eight mutants (R92C, W90C, Y141C, T179C, W183C) showed no detectible fluorescent signal, and the remaining three (L126C, N128C, Q151C) had a decreased affinity when compared to wild type receptors. Using RB, [^{3}H]granisetron saturation binding showed a similar pattern of changes, suggesting that granisetron and G-FL adopt broadly similar orientations. To assess the suitability of this novel 5-HT$_3$ receptor fluorophore, we explored its use in FC and FP assays.

3.3. Purification of 5-HT$_3$ receptors

FP required purified 5-HT$_3$ receptor that was achieved using HEK 293T cells stably expressing an N-terminal fusion protein. Initial purifications used an N-terminal myc-tag, but the high abundance of endogenous *c*-myc proteins prevented efficient enrichment of the myc-tagged receptor by immunoprecipitation. Subsequent purifications with an N-terminal FLAG-tagged 5-HT$_3$ receptor were more successful. The purity and identity of the FLAG-tagged receptors was confirmed by Coomassie staining, Western blot and mass spectrometry of excised bands (Fig. 4A, *inset*). Quantification of purified 5-HT$_3$ receptors showed yields of 90 ± 19 μg mL^{-1} eluted protein (n = 4) from 1200 cm^2 (~3 × 10^5 cells/cm^2), which is ~83 pmol. This is the equivalent of ~10^6 binding sites/cell. Concentrations calculated from RB were slightly higher (~250 pmol/mg). These results show that it is possible to isolate purified 5-HT$_3$ receptor in quantities that are sufficient for biological applications.

3.4. Fluorescence polarization

G-FL displayed the highest affinity in radioligand competition assays, showed suitable fluorescence intensity, and had fluorescent properties that were compatible with the filters in our FP system (Table 1). Addition of 2 nM G-FL to increasing concentrations of purified 5-HT$_3$ receptor gave a saturable increase in FP (Fig. 4A). These data were fitted with Eq. (1) yielding a pK_d of 8.94 ± 0.07 (K_d = 1.15 nM, n = 6). In the presence of excess unlabeled ligand FP signals were reduced to background levels.

The binding affinity of G-FL was also calculated by the independent measurements of association and dissociation kinetics, according to Eq. (5). Association curves for G-FL were fitted with mono-exponential functions to give k_{obs} (Fig. 4B). Plotting k_{obs} against the receptor concentration produced a straight line fit that yielded k_{on} and k_{off} that gave a K_d of 0.4 nM (Eq. (5), Fig. 4C). The value for k_{on} calculated with this method was similar to the average value determined directly from k_{obs} values using Eq. (6) (1.39 × 10^7 M^{-1} s^{-1}). A direct measurement of dissociation by the addition of excess unlabeled competitive ligand to G-FL equilibrated cells was also monophasic, with k_{off} values (0.001 s^{-1}) that were similar to those determined from plots of k_{obs} against ligand concentration (Fig. 4D). These results show that fluorescent granisetron-derivatives are suitable for the measurements of ligand affinity and binding kinetics.

In the presence of 2 nM G-FL and 2 nM purified 5-HT$_3$ receptor, known competitive ligands (agonists and antagonists) reduced FP in a concentration-dependent manner (Fig. 4E and F, Table 2). FP

Table 2
Affinities of competitive ligands measured using FC, FP and RB.

	Fluorescence polarization[a]			Flow cytometry[b]			Radioligand binding[c]		
Compound	pK_i (M)	K_i (nM)	n	pK_i (M)	K_i (nM)	n	pK_i (M)	K_i (nM)	n
Antagonists									
Granisetron	8.35 ± 0.06	4.5	8	8.53 ± 0.05	2.9	4	9.02 ± 0.06	0.95	5
Palonosetron	8.52 ± 0.01	3.0	3	9.79 ± 0.21	0.2	4	9.71 ± 0.06	0.2	4
Tropisetron	8.31 ± 0.16	4.9	6	8.70 ± 0.04	2.0	4	8.68 ± 0.21	2.1	3
Agonists									
5-HT	6.74 ± 0.26	182	4	6.90 ± 0.02	126	3	6.85 ± 0.23	141	5
*m*CPBG	6.55 ± 0.06	282	6	6.96 ± 0.05	110	4	6.98 ± 0.18	105	5
Quipazine	8.02 ± 0.16	9.5	6	8.41 ± 0.01	3.9	4	8.90 ± 0.02	1.25	5
Controls									
ACh	NB	–	3	NB	–	4	NB	–	3
GABA	NB	–	3	NB	–	4	NB	–	3
Glycine	NB	–	4	NB	–	4	NB	–	3
Picrotoxin	NB	–	7	NB	–	4	NB	–	3

[a] FP assays used 2 nM G-FL.
[b] FC assays 10 nM G-FL.
[c] Radioligand competition 0.75 nM [^{3}H]granisetron. NB = no detectible binding.

A

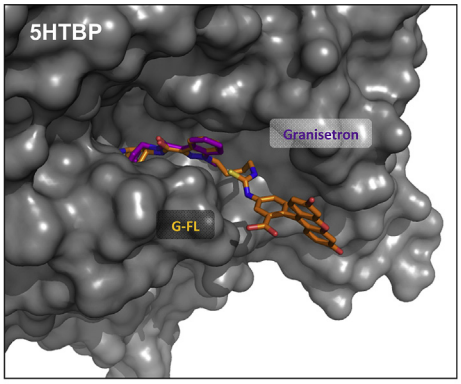

B

Receptor	Granisetron pK_i (M)	K_i (nM)	n	G-FL pK_d (M)	K_i (nM)	n
Wild Type	9.02 ± 0.06	0.95	5	8.49 ± 0.13	3.23	6
R92C	NB	-	4	NF	-	3
W90C	NB	-	6	NF	-	3
L126C	8.35 ± 0.16*	4.47	3	7.81 ± 0.12*	15.5	8
N128C	9.17 ± 0.18	0.68	4	8.09 ± 0.05*	8.91	7
Y141C	NB	-	3	NF	-	3
Q151C	9.21 ± 0.06	0.62	3	7.92 ± 0.19*	12.0	7
T179C	NB	-	3	NF	-	3
W183C	NB	-	6	NF	-	3

NB = No saturable binding measured using RB of [^{3}H]granisetron. NF = No saturable fluorescent signal using G-FL in FC assays. * Significantly different to wild type ($p > 0.05$, Students' T-test)

Fig. 3. A possible orientation of G-FL in the 5-HT$_3$ receptor orthosteric binding site. (A) G-FL (orange) is oriented using a pairwise alignment with the heteroaromatic rings of granisetron (purple) bound to the 5HTBP (gray surface) co-crystal structure (PDB: 2YME). In this orientation the fluorophore can be accommodated within the binding site. The pairwise alignment was made using PyMol v1.3 (Schrödinger LLC, OR, USA). (B) The effects of mutations on granisetron binding are the same as those reported elsewhere and similar to effects on G-FL.

was not reduced by either the Cys-loop receptor agonists ACh, GABA and glycine, or the non-competitive antagonist picrotoxin (PTX) at concentrations of up to 100 μM. These data show that 5-HT$_3$ receptor ligands specifically compete with G-FL at the orthosteric binding site, which can be used as a fluorescent probe for determining the affinities of non-labeled competitive ligands.

3.5. Flow cytometry

G-FL was also evaluated as a novel probe for FC. The results show that G-FL caused a specific dextral shift in the geometric mean when compared to similar experiments in the presence of excess unlabeled ligand or with untransfected HEK 293T cells (Fig. 5A). With G-FL a saturable increase in the geometric mean yielded a pK_d of 8.49 ± 0.12 (K_d = 3.23 nM, n = 6), similar to that determined in FP and RB. Also similar to FP, competition with known ligands and negative controls showed that the interaction was specific (Fig. 5B and C, Table 2), and the rate of dissociation of G-FL in the presence of excess non-labeled ligand was comparable (Fig. 5D). These results show that G-FL is also suitable for studying ligand binding with FC.

3.6. Radioligand measurements

To determine whether affinities measured using FC and FP were similar to those measured using a more established method we performed radioligand binding with [^{3}H]granisetron. Saturation binding with [^{3}H]granisetron and competition binding with known competitive ligands gave similar affinities to those measured using FC and FP (Fig. 6A *inset*, Table 2). Also consistent with FC and FP, at concentrations of up to 100 μM, binding was unaffected by the non-competitive ligand PTX, or the Cys-loop receptor agonists ACh, GABA or glycine (Fig. 6A–C, Table 2). Dissociation of [^{3}H]granisetron following the addition of excess unlabeled ligand gave a rate that was comparable to the values measured for G-FL using FC and FP (Fig. 6D). These results show that affinities measured using FC and FP are similar to those determined with radioligand binding.

3.7. In vivo localization of 5-HT$_3$ receptors

To further probe the utility of the new fluorescent probes we used *in vivo* imaging of anaesthetized mice injected with G-SiR, a compound with near-infrared emission. After 5 min (5 mg/kg i.p.), staining was visible in the gut, and by 20 min post-injection was also visible in salivary glands (Fig. 7A). Since the presence of 5-HT$_3$ receptors was not expected in salivary glands, further studies using dissected mouse salivary glands from sacrificed mice were performed.

To confirm the presence of 5-HT$_3$ receptors in these tissues Western blot analysis was undertaken using a 5-HT$_3$-specific antibody on total protein extracts from each of the identified organs (Fig. 7C). A clear band was seen in each, corresponding to the molecular weight expected for the 5-HT$_3$ receptor in Tris-Acetate gels. No band was seen in skeletal muscle which was used as a negative control. These results show that G-SiR is suitable for *in vivo* imaging where it specifically labels 5-HT$_3$ receptors.

4. Discussion

We report the synthesis of high affinity fluorescent 5-HT$_3$ receptor antagonists to create a series of ligands that cover a broad fluorescent spectrum from blue to near-infrared emission. We describe the application of G-FL in FC and FP, showing that it is possible to determine accurate and reproducible ligand binding affinities and kinetic parameters. As predicted from its spectroscopic properties, G-SiR gave clear staining *in vivo*, that was consistent with the known tissue distribution of 5-HT$_3$ receptors. These results are consistent with the specific, displaceable binding that we observed in radioligand binding assays and with previously reported specific binding of other fluorescent granisetron-derivatives using confocal microscopy (Simonin et al., 2012). As such, our study demonstrates the utility of novel fluorescent 5-HT$_3$ receptor ligands across a range of highly applicable pharmacological approaches.

Nanomolar affinities for our fluorescently labeled granisetron derivatives at the 5-HT$_3$ receptor were shown (Table 1). Coupling of fluorescein to the N1 position caused no apparent change in affinity when compared to the parent ligand granisetron. This is consistent with previous reported structure–activity relationships (Vernekar et al., 2010). The effects of mutations on granisetron binding were also consistent with previous studies that reported substitutions at R92, W90, T179, Y141 and W183 strongly affected binding, while mutations at L126, N128 and Q151 had only minimal effects (Beene et al., 2004; Price et al., 2008; Thompson et al., 2008, 2011). The magnitude by which the affinities of granisetron and G-FL changed following substitution differed (~3-fold for L126C, 13-fold for N128C and 19-fold for Q151C) and shows there are some differences in their binding, but the pattern of changes was similar for both ligands suggesting that they occupy broadly similar positions within the binding site. An alignment of the granisetron moiety of G-FL with granisetron bound to 5-HTBP (Fig. 3) supports this

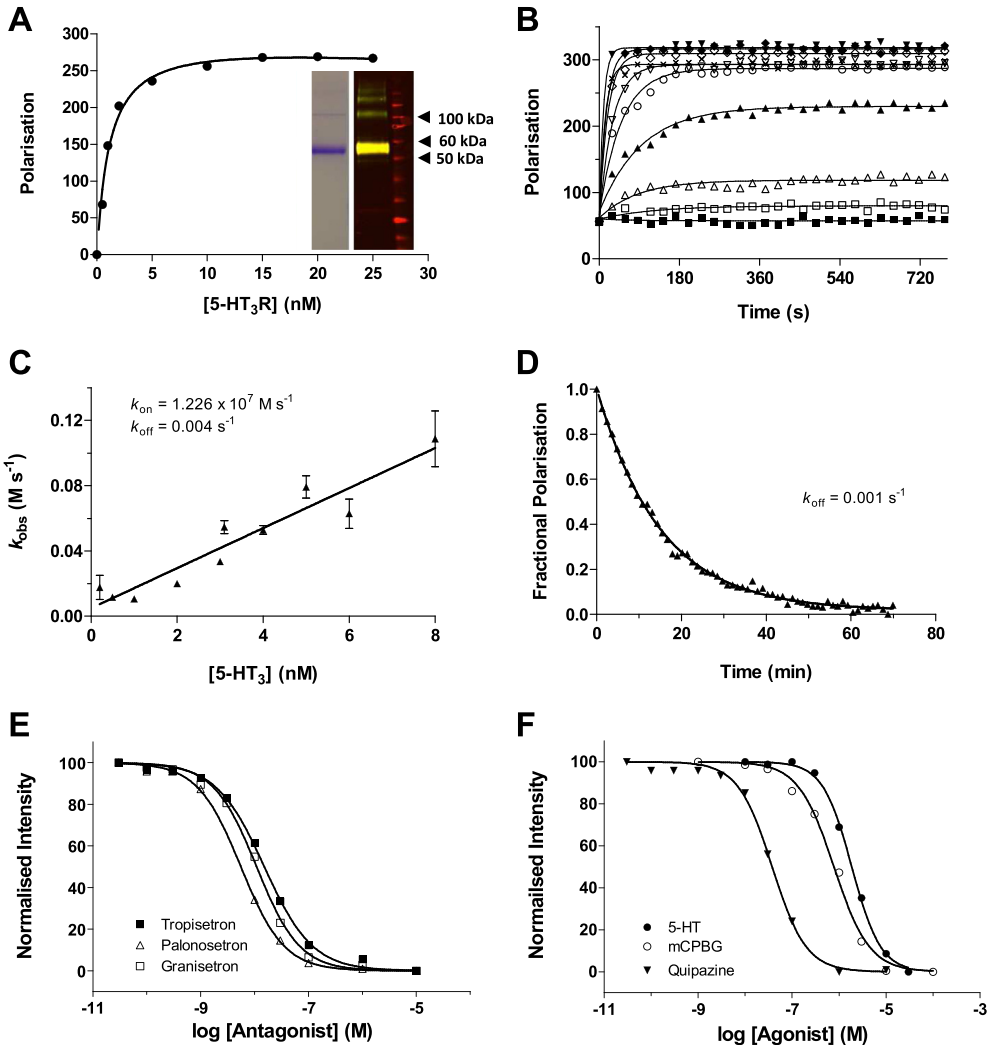

Fig. 4. Characterization of G-FL. (A) Saturation binding of G-FL using FP; *Inset*, visualization of FLAG-purified 5-HT_3 receptor with colloidal Coomassie staining (left) and Western blot analysis (right) using goat anti-FLAG/donkey anti-goat IRDye 800CW (green) and mouse anti-myc/donkey anti-mouse IRDye 680CW (red). The overlay of these two colors is yellow and a band at 55 kDa in the right lane corresponds to a 5-HT3A subunit monomer which displays both FLAG and myc epitopes. Weaker bands above 110 kDa are also seen following purification. (B) Association of G-FL at different concentrations of the 5-HT_3 receptor was measured using FP. Data points were fitted with a mono-exponential function to yield k_{obs}. (C) Linear regression was used to fit k_{obs} against the G-FL concentration to give k_{on} (slope) and k_{off} (y intercept at $x = 0$). (D) Dissociation of G-FL was measured following the addition of excess unlabeled ligand at $t = 0$ to G-FL equilibrated 5-HT_3 receptors. (E) Competition of varied concentrations of known 5-HT_3 receptor antagonists with 2 nM G-FL. (F) Competition with varied concentration of 5-HT_3 receptor agonists. Panels D, E and F traces are single experiments, but are representative of the larger dataset summarized in the text and Table 2. In panel B the symbols refer to values for no G-FL (■) or 0.2 nM (□), 0.5 nM (△), 1 nM (▲), 2 nM (○), 3 nM (▽), 4 nM (◊), 5 nM (×), 6 nM (◆) and 8 nM (▼) G-FL.

hypothesis, as the conjugated fluorophore is not sterically restricted in this orientation (Kesters et al., 2013). Also, the relatively high fluorescence polarization for the receptor-bound G-FL ligand suggests that fluorescein has a low degree of rotational movement, as expected in the tightly enclosed environment of the 5-HT_3 receptor ligand binding site.

G-FL had the highest affinity that was consistently shown with all three techniques described here (FC, 3.23 nM; FP, 1.14 nM; RB, 1.90 nM). Similar affinities have been reported for the parent granisetron molecule elsewhere (Thompson and Lummis, 2007) and association (k_{on} = 1.2 × 10^7 M^{-1} s^{-1}) and dissociation (k_{off} ~ 0.004 s^{-1}) rates of G-FL were also comparable to those reported for granisetron at similar temperatures (Hope et al., 1996; Rojas et al., 2008; Steward et al., 1995; Wong et al., 1995). Both k_{obs} and k_{off} were best fitted with single components, which is consistent with the single population of binding sites (A+A−) that is present in homomeric 5-HT_3 receptors (Hope et al., 1996; Lochner and Lummis, 2010; Miles et al., 2013; Thompson et al., 2011). As the dissociation rates measured by of FC and RB were similar, we can conclude that association rates were also comparable, given the similar affinities and the simple relationship between k_{off}, k_{on} and K_d (Eq. (5)). FC and FP competition on purified 5-HT_3 receptors also provided affinities for several unlabeled 5-HT_3 receptor agonists and competitive antagonists that had the same values and rank order as RB competition assays. This supports the utility of G-FL for pharmacological measurements that were facilitated by the large changes in fluorescence intensity and polarization that provided an excellent signal to noise ratio. As all of the methods accurately reported binding properties there appears to be no adverse influence from using receptors that are detergent-solubilized (FP), within crude cell homogenates (RB) or expressed on the surface of live cells (FC).

Here, we utilized the stable expression of FLAG/myc double-tagged 5-HT_3 receptors in HEK 293T cells using a lentiviral

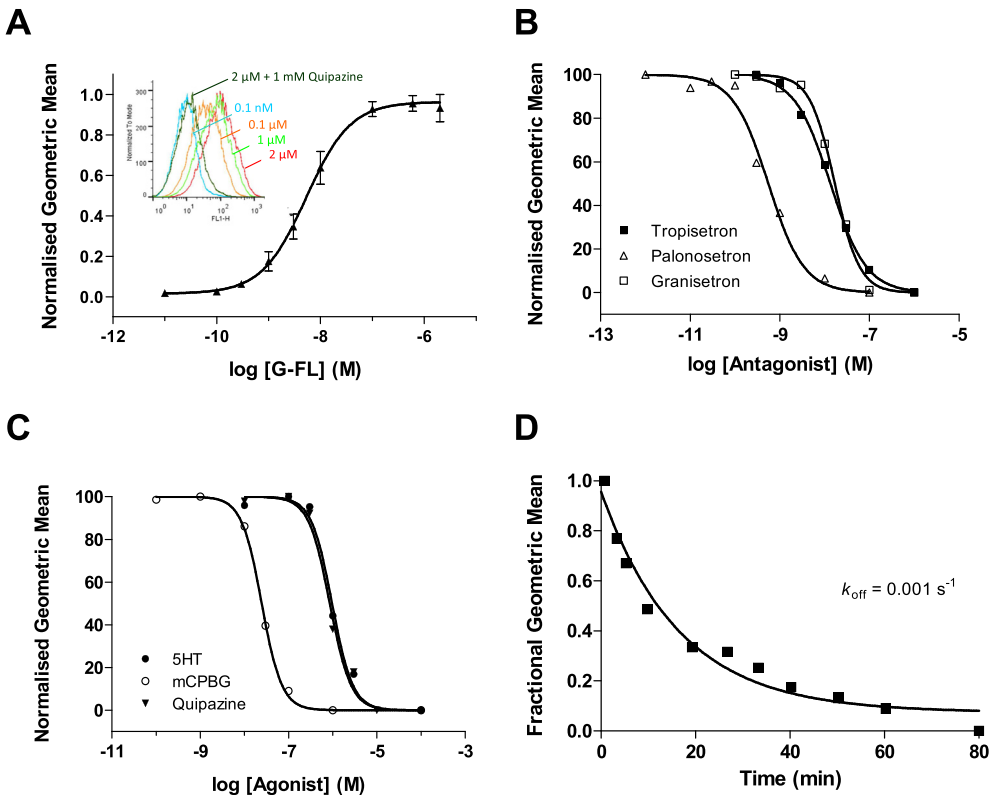

Fig. 5. 5-HT$_3$ receptor pharmacology measured with flow cytometry. (A) Saturation binding of G-FL determined using the shift in geometric mean. *Inset* fluorescence intensity distributions used to plot the binding curve (labels show the G-FL concentrations). (B) Competition binding of varied concentrations of known 5-HT$_3$ receptor antagonists with 10 nM G-FL. (C). Competition with known 5-HT$_3$ receptor agonists. (D) Dissociation of G-FL was measured following the addition of excess unlabeled ligand at $t = 0$ to G-FL equilibrated cells. Panels B, C and D are single experiments, but are representative of the larger dataset summarized in the text and Table 2.

system. Affinity purification over the N-terminal FLAG tag yielded up to ~90 µg mL^{-1} of purified protein from 1200 cm^2 of cells (3×10^5 cells/cm^2) grown in monolayers. This is ~83 pmol of purified receptors and the equivalent of ~10^6 binding sites/cell, which compares well with other studies (Dostalova et al., 2010; Hassaine et al., 2013). These receptors had intact binding sites with a pharmacology matching that of 5-HT$_3$ receptors described elsewhere (Brady et al., 2001; Thompson and Lummis, 2007). Mass spectrometry analysis gave a fragment pattern with 80% coverage of the 5-HT$_3$ receptor making its identification unequivocal. Purification of the mouse 5-HT$_3$ receptor was recently reported and also gave good yields using an N-terminal strep-tag, and poor yields with a C-terminal His$_{10}$ (Hassaine et al., 2013). Based on the gel images in Hassaine et al. (2013) the purity of their receptor was comparable to ours following a single step purification and similarly displayed a higher molecular weight impurity that was identified as binding immunoglobulin protein (BIP). Elsewhere, higher molecular weight bands have been suggested to be glycosylated and calnexin-associated 5-HT$_3$ receptors (Boess et al., 1992; Hovius et al., 1998). In our preparation, the two higher molecular weight bands were both labeled by anti-FLAG and anti-myc antibodies, suggesting that they both contain 5-HT$_3$ receptor proteins (Hovius et al., 1998), a hypothesis that was supported by the identification of 5-HT$_3$ receptors using mass spectrometry of these bands. In contrast to the findings of Hassaine et al. (2013) and ourselves, the successful purification of the C-terminal His$_6$-tagged purified mouse 5-HT$_3$ receptor was reported by Schmid et al. (1998) and Tairi et al. (1998), where it was immobilized on a quartz glass surface and used with fluorescein labeled GR119566X in real-time ligand binding assays. The use of His$_6$ was also reported following bacterial expression and purification of a fusion protein of 5-HT$_3$ receptor with a bacteriophage envelope protein and a C-terminal tag (Na et al., 2013). Our experiments using an anti-c-myc affinity gel were unsuccessful because of the high abundance of endogenous c-myc protein in 293T cells. These different results highlight the diversity of possible tags and the need to determine the appropriate one in each experimental system.

We have shown here that two different fluorescent methods (FC and FP) provide consistent measurements of binding affinity and kinetics that are comparable to values from more traditional methods such as radioligand binding. Previously we have demonstrated the utility of these 5-HT$_3$ receptor ligands for visualizing the specific labeling of cell-surface receptors using confocal microscopy (Simonin et al., 2012). Using a different fluorescent approach to study 5-HT$_3$ receptor pharmacology, Thompson et al. (2010b) have also described the use of a voltage-sensitive fluorescent dye. In these studies the voltage-sensitive dye reported functional responses and was consequently able to probe the actions of both competitive and non-competitive ligands. In contrast, the FC and FP assays reported here are more limited as they focus on a single binding site (similar to RB). However, they can easily be adapted to high-throughput methods and, as such, provide an ideal accompaniment to voltage-sensitive dyes in high-throughput screening programs. Of the two fluorescent methods described here, FC was the simplest as it required only standard cell-culture materials, could be performed on live cells, and provided time- and cost-efficient measurements that were reliable, reproducible and could be readily adapted to multi-well formats. Another fluorescent probe within our series (G-SiR) emitted in the near-IR region of the spectrum and was ideal for *in vivo* studies since the longer

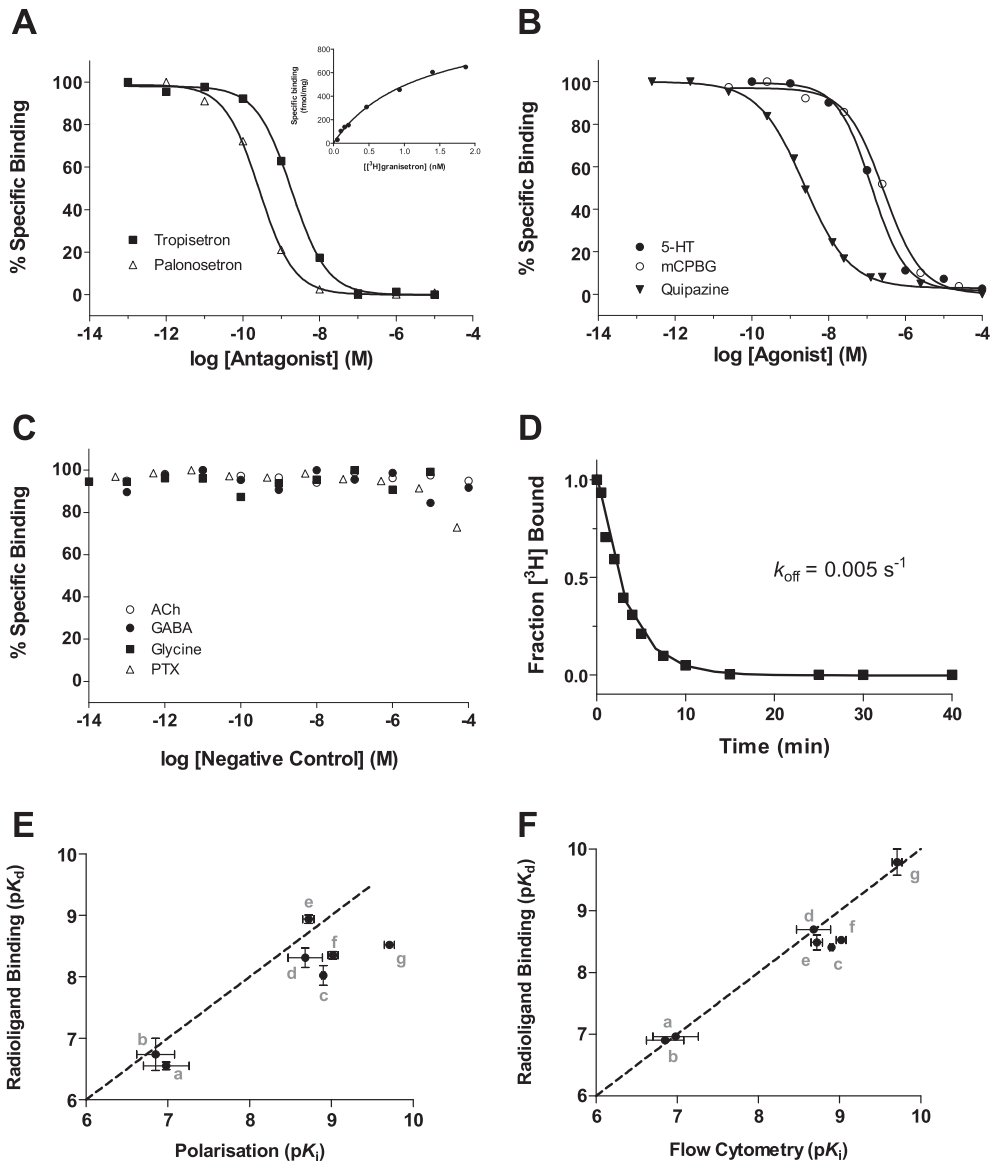

Fig. 6. Radioligand saturation and competition binding. (A) Competition between 0.75 nM [^{3}H]granisetron and varied concentration of 5-HT$_3$ receptor antagonists; *Inset*, saturation binding of the radiolabeled probe [^{3}H]granisetron. (B) Competition binding of [^{3}H]granisetron with known 5-HT$_3$ receptor agonists. (C) There was no competition with ligands that are agonists of other Cys-loop receptors or the non-competitive antagonist picrotoxin (PTX). (D) Dissociation of the granisetron following the addition of excess unlabeled ligand. The dissociation rate of [^{3}H]granisetron was similar to rates measured for G-FL in FC and FP assays, consistent with the similar affinities of the two ligands. (E) A comparison of binding affinities determined using FP and RB. (F) A comparison of binding affinities measured with FC and RB; (a) *m*CPBG; (b) 5-HT; (c) quipazine; (d) tropisetron; (e) G-FL; (f) granisetron; (g) palonosetron. The dashed line is unity. The values are from Tables 1 and 2. Panels A, B, C and D are single experiments, but are representative of the larger dataset summarized in the text and Table 2.

wavelengths have reduced phototoxicity, give deeper tissue penetration and are further from the auto-fluorescence that is often seen in biological tissues (Lukinavičius et al., 2013). In our studies the presence of 5-HT$_3$ receptors in mammalian brain and gut was expected as it is known to be widely distributed in these regions (Barnes et al., 2009; Niesler et al., 2003), but its presence in salivary gland is not as well reported (Perren et al., 1995). Also, while serotonin is known to be present in salivary glands, there is evidence for the role of metabotropic 5-HT receptors, rather than the ionotropic 5-HT$_3$ receptor (Turner et al., 1996). The physiological function of these receptors is therefore currently unknown and requires further work. Other fruitful avenues of research may also use acridone and 5-TAMRA conjugated ligands as these are highly photostable and have been used for confocal and high resolution techniques such as two photon excitation (Banala et al., 2012; Puliti et al., 2011; Reymond et al., 1996). Thiazole orange (TO) is known to self-quench owing to stacking, but emits light when the stacking is disrupted by binding (Lukinavičius and Johnsson, 2011; Volkova et al., 2008), a property that gives low background fluorescence and we found preliminary evidence of when using our ligand G-TO (unpublished data).

4.1. Summary

We report nanomolar affinity fluorescent 5-HT$_3$ receptor ligands with absorption and emission that cover a wide range of the fluorescent spectrum. We show they occupy the 5-HT$_3$ receptor orthosteric binding site and the highest affinity fluorescein-containing ligand can be utilized in FC and FP to probe this region. The fluorescent changes of all of our ligands offer excellent

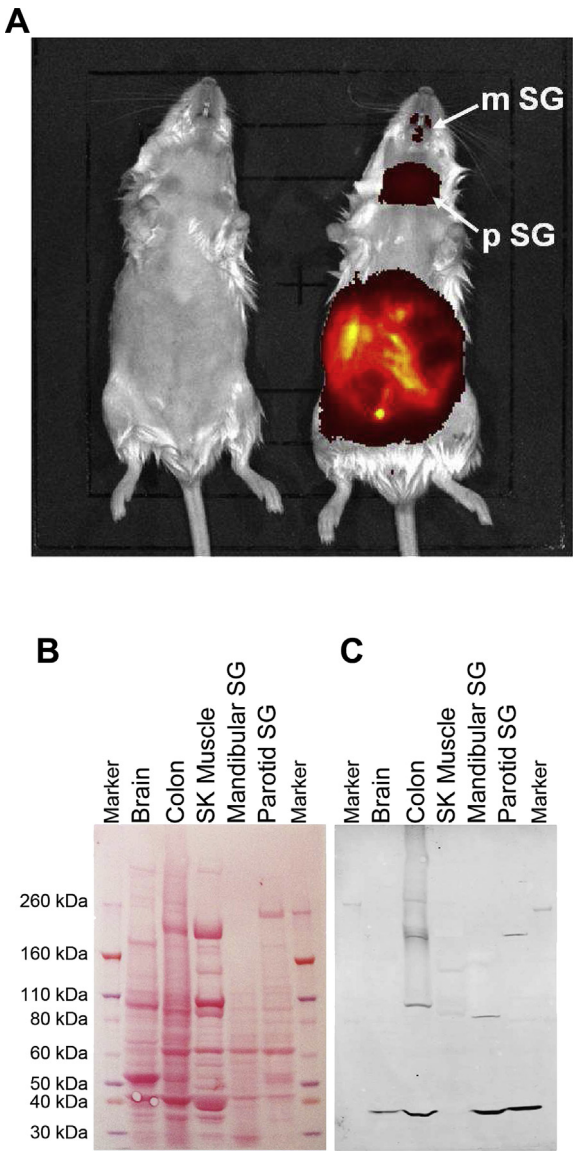

Fig. 7. Characterization of 5-HT_3 receptors in mouse tissues. (A) *In vivo* imaging of G-SiR (5 mg/kg, i.p.) after injection into anaesthetized C57BL male mice. Representative image of control (left) and injected (right) mice after 20 min. Strong fluorescence is visible in the abdominal cavity showing intestine, but also in salivary glands (as evidenced by subsequent dissection). Mandibular (m) and parotid (p) salivary glands (SG), respectively, are indicated by arrows. (B) Ponceau staining of total protein extracts (37.5 μg) from mouse tissues. (C) Visualization of 5-HT3A receptor subunits with goat anti-5-HT_3 followed by Donkey anti-Goat IRDye800CW. A clear band was visible at the size expected for the 5-HT3A subunit. The gel shown is a representative example of three other similar gels. SK = skeletal (muscle); SG = salivary gland.

signal to noise ratios, and the measured affinities and binding kinetics are reproducible and reliable, making them ideally suited for pharmacological studies or as an alternative to antibodies that are not able to penetrate tissues *in vivo*.

Acknowledgments

We thank Prof. John Peters for providing the 5-HT_3 receptor subunit cDNA and Prof. Oliver Mühlemann for kindly providing lab space for MDR. We thank Prof. Roch-Philippe Charles for assistance with mouse experiments. This work was supported by the Swiss National Science Foundation [SNSF-professorship PP00P2_146321/1 to ML]. MDR was supported by a Sinergia grant from the Swiss National Science Foundation [CRSII3-136222], the NOMIS Foundation and the HOLCIM Stiftung zur Förderung der wissenschaftlichen Fortbildung.

Appendix A. Supplementary data

Supplementary data related to this article can be found at http://dx.doi.org/10.1016/j.neuropharm.2014.11.007.

References

Banala, S., Maurel, D., Manley, S., Johnsson, K., 2012. A caged, localizable rhodamine derivative for superresolution microscopy. ACS Chem. Biol. 7, 289–293.
Barnes, N.E., Hales, T.G., Lummis, S.C.R., Peters, J.A., 2009. The 5-HT_3 receptor – the relationship between structure and function. Neuropharmacology 56, 273–284.
Beene, D.L., Price, K.L., Lester, H.A., Dougherty, D.A., Lummis, S.C.R., 2004. Tyrosine residues that control binding and gating in the 5-Hydroxytryptamine$_3$ receptor revealed by unnatural amino acid mutagenesis. J. Neurosci. 24, 9097–9104.
Bermudez, J., Fake, C.S., Joiner, G.F., Joiner, K.A., King, F.D., Miner, W.D., Sanger, G.J., 1990. 5-Hydroxytryptamine (5-HT_3) receptor antagonists. 1. Indazole and Indolizine-3-carboxylic acid derivatives. J. Med. Chem. 33, 1924–1929.
Boess, F.G., Lummis, S.C.R., Martin, I.L., 1992. Molecular properties of 5-Hydroxytryptamine$_3$ receptor-type binding sites purified from NG108-15 cells. J. Neurochem. 59, 1692–1701.
Brady, C.A., Stanford, I.M., Ali, I., Lin, L., Williams, J.M., Dubin A, E., Hope, A.G., Barnes, N.M., 2001. Pharmacological comparison of human homomeric 5-HT_{3A} receptors versus heteromeric 5-$HT_{3A/3B}$ receptors. Neuropharmacology 41, 282–284.
Clark, R.D., Miller, A.B., Berger, J., Repke, D.B., Weinhardt, K.K., Kowalczyk, B.A., Eglen, R.M., Bonhaus, D.W., Lee, C.H., 1993. 2-(Quinuclidin-3-yl)pyrido[4,3-*b*]indol-1-ones and Isoquinolin-1-ones. Potent conformationally restricted 5-HT_3 receptor Antagonists. J. Med. Chem. 36, 2645–2657.
Dostalova, Z., Liu, A., Zhou, X., Farmer, S.L., Krenzel, E.S., Arevalo, E., Desai, R., Feinberg-Zadek, P.L., Davies, P.A., Yamodo, I.H., Forman, S.A., Miller, K.W., 2010. High-level expression and purification of Cys-loop ligand-gated ion channels in a tetracycline-inducible stable mammalian cell line: $GABA_A$ and serotonin receptors. Protein Sci. 19, 1728–1738.
Egawa, T., Hanaoka, K., Koide, Y., Ujita, S., Takahashi, N., Ikegaya, Y., Matsuki, N., Terai, T., Ueno, T., Komatsu, T., Nagano, T., 2011. Development of a far-red to near-infrared fluorescence probe for calcium ion and its application to multicolor neuronal imaging. J. Am. Chem. Soc. 133, 14157–14159.
Hassaine, G., Deluz, C., Li, X.-D., Graff, A., Vogel, H., Nury, H., 2013. Large scale expression and purification of the mouse 5-HT3 receptor. Biochim. Biophys. Acta 1828, 2544–2552.
Hill, A.V., 1909. The mode of action of nicotine and curari, determined by the form of the contraction curve and the method of temperature coefficients. J. Physiol. 39, 361–373.
Holzhauser, C., Berndl, S., Menacher, F., Breunig, M., Göpferich, A., Wagenknecht, H.-A., 2010. Synthesis and optical properties of cyanine dyes as fluorescent DNA base substitutions for live cell imaging. Eur. J. Org. Chem. 2010, 1239–1248.
Hope, A.G., Peters, J.A., Brown, A.M., Lambert, J.J., Blackburn, T.P., 1996. Characterization of a human 5-hydroxytryptamine$_3$ receptor type A (h5-HT_3R-A_S) subunit stably expressed in HEK 293 cells. Br. J. Pharmacol. 118, 1237–1245.
Hovius, R., Tairi, A.P., Blasey, H., Bernard, A., Lundstrom, K., Vogel, H., 1998. Characterization of a mouse serotonin 5-HT_3 receptor purified from mammalian cells. J. Neurochem. 70, 824–834.
Kesters, D., Thompson, A.J., Brams, M., van Elk, R., Spurny, R., Geitmann, M., Villalgordo, J.M., Guskov, A., Helena Danielson, U., Lummis, S.C.R., Smit, A.B., Ulens, C., 2013. Structural basis of ligand recognition in 5-HT_3 receptors. EMBO Rep. 14, 49–56.
Kvach, M.V., Stepanova, I.A., Prokhorenko, I.A., Stupak, A.P., Bolibrukh, D.A., Korshun, V.A., Shmanai, V.V., 2009. Practical synthesis of isomerically pure 5- and 6-carboxytetramethylrhodamines, useful dyes for DNA probes. Bioconjug. Chem. 20, 1673–1682.
Langlois, M., Soulier, J.L., Yang, D., Bremont, B., Florac, C., Rampillon, V., Giudice, A., 1993. Structural analysis of 5-HT_3 receptor antagonists: synthesis and pharmacological activity of various aromatic esters or amides derived from tropane and 1,2,6-trisubstituted piperidine. Eur. J. Med. Chem. 28, 869–880.
Lavis, L.D., Raines, R.T., 2008. Bright ideas for chemical biology. ACS Chem. Biol. 3, 142–155.
Lochner, M., Lummis, S.C.R., 2010. Agonists and antagonists bind to an A-A interface in the heteromeric 5-HT_3AB receptor. Biophys. J. 98, 1494–1502.
Lukinavičius, G., Johnsson, K., 2011. Switchable fluorophores for protein labeling in living cells. Curr. Opin. Chem. Biol. 15, 768–774.
Lukinavičius, G., Umezawa, K., Olivier, N., Honigmann, A., Yang, G., Plass, T., Mueller, V., Reymond, L., Corrêa Jr., I.R., Luo, Z.-G., Schultz, C., Lemke, E.A., Heppenstall, P., Eggeling, C., Manley, S., Johnsson, K., 2013. A near-infrared fluorophore for live-cell super-resolution microscopy of cellular proteins. Nat. Chem. 5, 132–139.

Miles, T.F., Dougherty, D.A., Lester, H.A., 2013. The 5-HT_3AB receptor shows an A_3B_2 stoichiometry at the plasma membrane. Biophys. J. 105, 887–898.
Moore, N.A., Sargent, B.J., Manning, D.D., Guzzo, P.R., 2013. Partial agonism of 5-HT_3 receptors: a novel approach to the symptomatic treatment of IBS-D. ACS Chem. Neurosci. 4, 43–47.
Na, J.-H., Shin, J., Jung, Y., Lim, D., Shin, Y.-K., Yu, Y.G., 2013. Bacterially expressed human serotonin receptor 3A is functionally reconstituted in proteoliposomes. Protein Expr. Purif. 88, 190–195.
Niesler, B., Frank, B., Kapeller, J., Rappold, G.A., 2003. Cloning, physical mapping and expression analysis of the human 5-HT_3 serotonin receptor-like genes *HTR3C, HTR3D* and HTR3E. Gene 310, 101–111.
Perren, M.J., Rogers, H., Mason, G.S., Bull, D.R., Kilpatrick, G.J., 1995. A pharmacological comparison of [^{3}H]-granisetron binding sites in brain and peripheral tissues of the mouse. Naunyn Schmiedeb. Arch. Pharmacol. 351, 221–228.
Price, K.L., Bower, K.S., Thompson, A.J., Lester, H.A., Dougherty, D.A., Lummis, S.C.R., 2008. A hydrogen bond in loop A is critical for the binding and function of the 5-HT_3 receptor. Biochemistry 47, 6370–6377.
Privé, G.G., 2007. Detergents for the stabilization and crystallization of membrane proteins. Methods 41, 388–397.
Puliti, D., Warther, D., Orange, C., Specht, A., Goeldner, M., 2011. Small photoactivatable molecules for controlled fluorescence activation in living cells. Biorg. Med. Chem. 19, 1023–1029.
Reymond, J.L., Koch, T., Schröer, J., Tierney, E., 1996. A general assay for antibody catalysis using acridone as a fluorescent tag. Proc. Natl. Acad. Sci. U. S. A. 93, 4251–4256.
Rojas, C., Stathis, M., Thomas, A.G., Massuda, E.B., Alt, J., Zhang, J., Rubenstein, E., Sebastiani, S., Cantoreggi, S., Snyder, S.H., Slusher, B., 2008. Palonosetron exhibits unique molecular interactions with the 5-HT_3 receptor. Anesth. Analg. 107, 469–478.
Schmid, E.L., Tairi, A.-P., Hovius, R., Vogel, H., 1998. Screening ligands for membrane protein receptors by total internal reflection fluorescence: the 5-HT_3 serotonin receptor. Anal. Chem. 70, 1331–1338.
Simonin, J., Vernekar, S.K.V., Thompson, A.J., Hothersall, J.D., Connolly, C.N., Lummis, S.C.R., Lochner, M., 2012. High-affinity fluorescent ligands for the 5-HT_3 receptor. Bioorg. Med. Chem. Lett. 22, 1151–1155.
Steward, L.J., Ge, J., Bentley, K.R., Barber, P.C., Hope, A.G., Lambert, J.J., Peters, J.A., Blackburn, T.P., 1995. Evidence that the atypical 5-HT_3 receptor ligand, [^{3}H]-BRL46470, labels additional 5-HT_3 binding sites compared to [^{3}H]-granisetron. Br. J. Pharmacol. 116, 1781–1788.
Tairi, A.-P., Hovius, R., Pick, H., Blasey, H., Bernard, A., Surprenant, A., Lundström, K., Vogel, H., 1998. Ligand binding to the serotonin 5HT_3 receptor studied with a novel fluorescent ligand. Biochemistry 37, 15850–15864.
Thompson, A.J., Lester, H.A., Lummis, S.C.R., 2010a. The structural basis of function in Cys-loop receptors. Q. Rev. Biophys. 43, 449–499.
Thompson, A.J., Lochner, M., Lummis, S.C.R., 2008. Loop B is a major structural component of the 5-HT_3 receptor. Biophys. J. 95, 5728–5736.
Thompson, A.J., Lummis, S.C.R., 2007. The 5-HT_3 receptor as a therapeutic target. Expert Opin. Ther. Targets 11, 527–540.
Thompson, A.J., Lummis, S.C.R., 2013. Discriminating between 5-HT_3A and 5-HT_3AB receptors. Br. J. Pharmacol. 169, 736–747.
Thompson, A.J., Price, K.L., Lummis, S.C.R., 2011. Cysteine modification reveals which subunits form the ligand binding site in human heteromeric 5-HT_3AB receptors. J. Physiol. 589, 4243–4257.
Thompson, A.J., Verheij, M.H.P., Leurs, R., De Esch, I.J.P., Lummis, S.C.R., 2010b. An efficient and information-rich biochemical method design for fragment library screening on ion channels. Biotechniques 49, 822–829.
Turner, J.T., Sullivan, D.M., Rovira, I., Camden, J.M., 1996. A regulatory role in mammalian salivary glands for 5-Hydroxytryptamine receptors coupled to increased cyclic AMP production. J. Dent. Res. 75, 935–941.
Vernekar, S.K.V., Hallaq, H.Y., Clarkson, G., Thompson, A.J., Silvestri, L., Lummis, S.C.R., Lochner, M., 2010. Toward biophysical probes for the 5-HT_3 receptor: structure–activity relationship study of granisetron derivatives. J. Med. Chem. 53, 2324–2328.
Volkova, K.D., Kovalska, V.B., Balanda, A.O., Losytskyy, M.Y., Golub, A.G., Vermeij, R.J., Subramaniam, V., Tolmachev, O.I., Yarmoluk, S.M., 2008. Specific fluorescent detection of fibrillar α-synuclein using mono- and trimethine cyanine dyes. Biorg. Med. Chem. 16, 1452–1459.
Walstab, J., Rappold, G., Niesler, B., 2010. 5-HT_3 receptors: role in disease and target of drugs. Pharmacol. Ther. 128, 146–169.
Wiznerowicz, M., Trono, D., 2003. Conditional suppression of cellular genes: lentivirus vector-mediated drug-inducible RNA interference. J. Virol. 77, 8957–8961.
Wong, E.H.F., Clark, R., Leung, E., Loury, D., Bonhaus, D.W., Jakeman, L., Parnes, H., Whiting, R.L., Eglen, R.M., 1995. The interaction of RS 25259-197, a potent and selective antagonist, with 5-HT_3 receptors, in vitro. Br. J. Pharmacol. 114, 851–859.
Wysocki, L.M., Lavis, L.D., 2011. Advances in the chemistry of small molecule fluorescent probes. Curr. Opin. Chem. Biol. 15, 752–759.